

Evaluation of Plasma-Sprayed Tungsten for Fusion Reactors

R.A. Neiser, G.R. Smolik, K.J. Hollis, and R.D. Watson

Tungsten coatings are being considered for a variety of uses inside fusion reactors. Measurements of several properties of vacuum plasma-sprayed tungsten important for fusion energy applications are reported. Of vital concern is the thermal conductivity of the sprayed tungsten. Over the temperature range 25 to 1500 °C, the thermal conductivity was approximately 60% of the value for high-purity tungsten. Of greater importance to reactor safety is the reactivity of tungsten with steam. It was found that the volatilization and reaction rates of plasma-sprayed tungsten from 800 to 1200 °C are similar to hot rolled tungsten. Several other useful properties have also been reported. The elastic constants of the sprayed tungsten were measured ultrasonically. The deposits were anisotropic; for example, the Young's modulus measured in a direction parallel to the substrate was greater than that measured in the direction perpendicular to it, and their elastic moduli were approximately 30% lower than tabulated values for bulk tungsten. The average bulk density of the sprayed tungsten was approximately 17.4 g/cm³, which is 90% of the theoretical density.

1. Introduction

TUNGSTEN is a candidate material for high heat flux, plasma-facing components (PFCs) in fusion reactors such as the International Thermonuclear Experimental Reactor (ITER). Plasma spraying is being considered for producing coatings on substrate materials and repairing *in situ* erosion losses due to plasma interactions. This article describes an investigation conducted on vacuum plasma sprayed tungsten for such applications.

Deposits were produced on different substrate materials at Sandia National Laboratories (SNL) in a low-pressure plasma spray system. These deposits were characterized with regard to density and microstructures observed by optical metallography of etched specimens. The amounts of oxides and other contaminants in the deposits were determined by x-ray diffraction, x-ray fluorescence, and oxygen analysis. The elastic constants of the deposits were measured ultrasonically.

The microstructures of the deposits were correlated with measured properties critical to some of the operational and safety aspects of a fusion reactor. The properties that were measured include thermal conductivity from room temperature to 1500 °C and the reactivity with high-temperature steam.

The thermal conductivity of the sprayed materials on plasma-facing components is important because it controls the temperature gradient and therefore the surface temperature of components during reactor operations. The thermal conductivity of tungsten coatings removed from copper and stainless steel

substrates was measured and compared to tabulated values for wrought tungsten.

The high-temperature steam tests are associated with fusion reactor safety considerations during a loss of coolant accident (LOCA). Volatilization of the tungsten oxides produced by the reaction of tungsten with high-temperature steam during an accident could potentially release radioactive tungsten isotopes. In addition, hydrogen produced from the reaction of tungsten with steam must be kept below the amount that could produce an explosive mixture. Data addressing both these concerns were obtained from deposits that were removed from substrates and tested in flowing steam at temperatures ranging from 800 to 1200 °C at the Idaho National Engineering Laboratory (INEL). This article presents comparisons of the reaction rates, i.e., hydrogen generation and volatility, of these deposits to pure wrought tungsten.

2. Specimen Preparation

The deposits were prepared by low-pressure plasma spraying. The spray parameters are given in Table 1. The feedstock powder was a 5 to 25 µm powder with an average size of 13.5 µm. The fine size was selected because of the high melting point of tungsten. A Plasmadyne SG-100* torch with a Mach I type 453 anode was used. Tungsten was sprayed onto graphite, copper, and stainless steel substrates. The tungsten deposited onto 25.4-mm diameter graphite pedestals was 3 to 4 mm thick. Poor bonding with the graphite caused the tungsten deposits to separate from the graphite during deposition and become distorted. Droplets did not strike the curled edges of these deposits at normal incidence, producing higher levels of porosity in these regions.

Tungsten coatings were also deposited on 24-mm square copper blocks for steam tests and 16-mm diameter copper and stainless steel buttons for thermal conductivity measurements.

Key Words: elastic constants, fusion reactors, low-pressure plasma processing, microstructure, steam tests, temperature application, thermal conductivity, tungsten

R.A. Neiser and R.D. Watson, Sandia National Laboratories, Albuquerque, NM 87185; **G.R. Smolik**, EG & G Idaho, Inc., Idaho National Engineering Laboratory, Idaho Falls, ID 83415; and **K.J. Hollis**, University of Wisconsin, Madison, WI 53706.

Published in the Proceedings of the 1993 National Thermal Spray Conference (NTSC '93), Anaheim, CA, June 7-11, 1993.

* Product of Miller Thermal, Appleton, WI 54912.

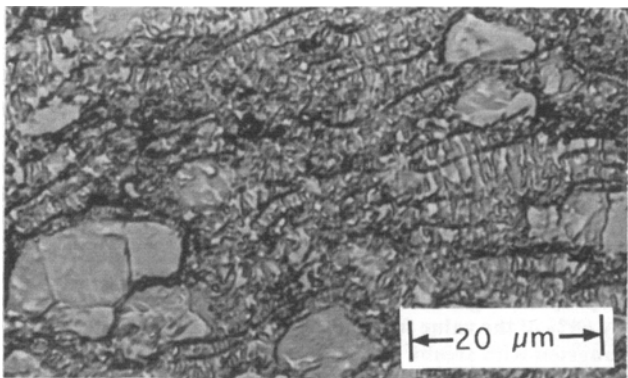


Fig. 1 Etched microstructure of low-pressure plasma-sprayed tungsten deposited on copper.

Table 1 Nominal spraying parameters

Current	800 A
Voltage.....	50.0 V
Input power.....	40.0 kW
Power lost to torch coolant.....	20.6 kW
Chamber pressure	200 torr
Primary gas (Ar)	46.2 L/min
Secondary gas (H ₂)	3.71 L/min
Carrier gas (Ar)	2.91 L/min
Standoff.....	110 mm
Feed rate	29 g/min

These samples were more uniform in thickness and more tightly bonded to their substrates than those on the graphite substrates. These coatings were 2.5-mm thick. All of the data reported here were collected on free-standing specimens. Free-standing coupons of tungsten were produced by machining away the copper or stainless steel. A 20% solution of nitric acid in ethanol was used to etch away any remaining copper. Residual stainless steel was removed by lapping. Specimens for thermal conductivity measurements were turned down to a final diameter of 12.7 mm and ground to a thickness of 2.0 mm. These specimens were polished to a 1-μm finish using diamond paste prior to testing.

Specimens for the steam experiments were tested in the as-sprayed condition to represent plasma-sprayed surfaces. No attempt was made to grind the deposits to improve surface quality, to provide more regularly shaped specimens, or to remove porous material concentrated near the edges. The reaction rates should be representative of plasma spray repairs inside of a fusion reactor that have not been subsequently ground or machined.

3. Experimental Results

3.1 Deposit Characterization

The soundness of the deposits was checked by various density and metallographic methods. Water immersion was used to measure the bulk densities of the specimens. Measurements were made both at SNL and INEL, and excellent agreement was obtained. The average bulk density for specimens sprayed onto

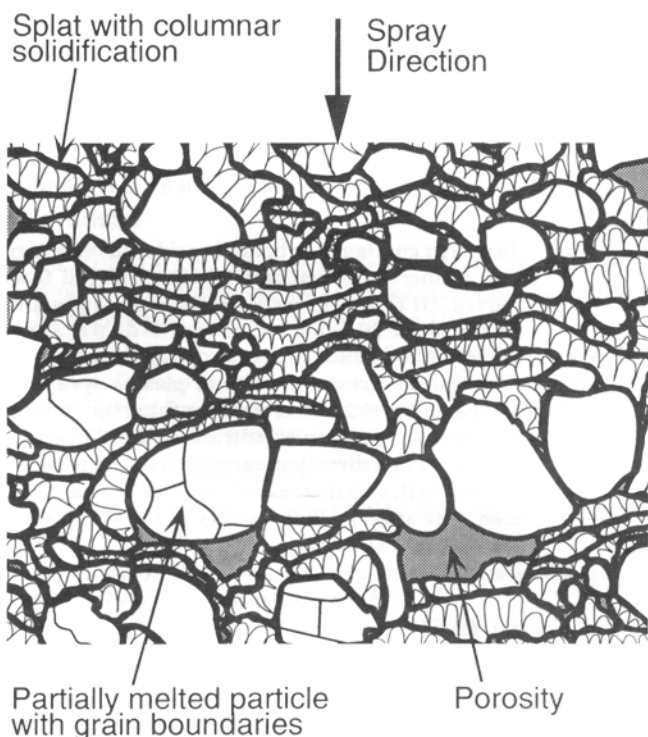


Fig. 2 Schematic diagram of the plasma-sprayed tungsten microstructure in Fig. 1.

graphite was 17.3 g/cm³ (89.6% of theoretical). The densities of tungsten sprayed onto copper and stainless steel were both 17.5 g/cm³ (90.7% of theoretical).

Metallography, in addition to the density data, provided a good characterization of the various types of deposits. Cross sections of the tungsten deposits from the graphite substrates exhibited porosity at the circumference where particle impact was not perpendicular to the substrate and contributed to the slightly lower density of these specimens. Optical metallography of polished cross sections revealed the presence of a few well-rounded pores, but no other microstructural features could be discerned. However, etching the specimens for 30 s in a solution of 10 g K₃Fe(CN)₆ and 10 g NaOH in 200 ml of distilled water revealed rich microstructure, as shown in Fig. 1. The important microstructural features of this micrograph are shown schematically in Fig. 2. A significant amount of the deposit is composed of partially melted tungsten particles. The high melting temperature of tungsten (3410 °C) makes it very difficult to melt, despite the fine size of the feedstock powder. Most of the pores occur next to the unmelted particles, and probably formed because the unmelted material could not flow on impact. An examination of the tungsten at higher magnifications in the scanning electron microscope (SEM) revealed the presence of very fine pores (<1 μm) at the boundaries between both melted and unmelted particles. Inside the flattened droplets (splats), a columnar microstructure was observed. This structure was previously observed by Moreau et al. in sprayed coatings of molybdenum.^[1] The microstructure results from the simultaneous nucleation and growth of many crystallites across the width of the splat. Moreau et al. have shown that in plasma-sprayed molybdenum the crystallites have the [100] direction oriented parallel to the direction

of heat removal. The orientation of the crystallites in the tungsten deposits was not measured, but because the plasma-sprayed microstructures of these two body-centered cubic refractory metals are so similar, it is also probably [100]. In another study, Sampath observed a [100] texture in vacuum plasma-sprayed nickel coatings.^[2]

The tungsten purity was examined by using x-ray diffraction to observe secondary phases, using x-ray fluorescence to examine chemical impurities, and by measuring the oxygen content with a Leco TC-136 Nitrogen/Oxygen Determinator*. X-ray diffraction of the feedstock powder and the sprayed deposits showed no indication of any minor phases. An x-ray fluorescence spectrum was taken from the polished surface of one of the specimens and exhibited essentially pure tungsten. Except for trace amounts of chromium and iron, no other contaminating elements having an atomic number greater than 10 were detected. The oxygen analysis showed that the feedstock powder and the deposit had an average oxygen content of 520 ppm by weight. Both specimens were measured four times. The 95% confidence intervals were 430 to 660 ppm for the powder and 510 to 530 ppm for the deposit. Passage of the particles through the argon/hydrogen plasma did not measurably reduce the oxygen content of the tungsten.

3.2 Reaction Rates in Steam

The samples were tested in flowing steam in the VAPOR (Volatilization of Activation Product Oxides Reactor) system.^[3] The samples were inductively heated in a quartz system. The

amounts of volatilized oxides were determined by weight change or by chemical analyses of the products deposited in the test chamber, quartz filter, and other components of the quartz test system. The quantities of hydrogen generated were determined by completely condensing steam from the gas stream and measuring the residual gas in an inverted graduated cylinder.

Tests were performed on two types of plasma-sprayed deposits—those produced on graphite and copper and also on a sample of pure hot rolled tungsten. The matrix of test temperatures and times is shown in Table 2. Tests between 800 and 1200 °C were conducted in a steam environment with a mass input of 0.03 g/s. Steam velocity at the specimen surfaces was approximately 0.05 m/s.

3.3 Steam Test Results

The volatilization and deposition of tungsten oxide products throughout the test system and in the quartz wool filter increased noticeably at 1000 °C and above. The amounts of product for these higher temperature tests were determined by gravimetric measurements. Due to the smaller amounts deposited in the 800 and 900 °C tests, however, determinations were made by dissolving the oxide product with a hydrofluoric and nitric acid mixture and analyzing the solutions with atomic emission spectroscopy/inductively coupled plasma (AES-ICP). The results

* Product of Leco, St. Joseph, MO.

Table 2 Summary of tungsten tests in steam

Form of tungsten	Sample	Temperature, °C	Time, min
Deposit on graphite	PSW2	800	60
	PSW5	900	60
	PSW1	1000	60
	PSW3	1100	60
	PSW4	1200	15
Deposit on copper	PSW8	800	60
	PSW9	1100	32
Hot rolled tungsten.....	PW1	1100	60

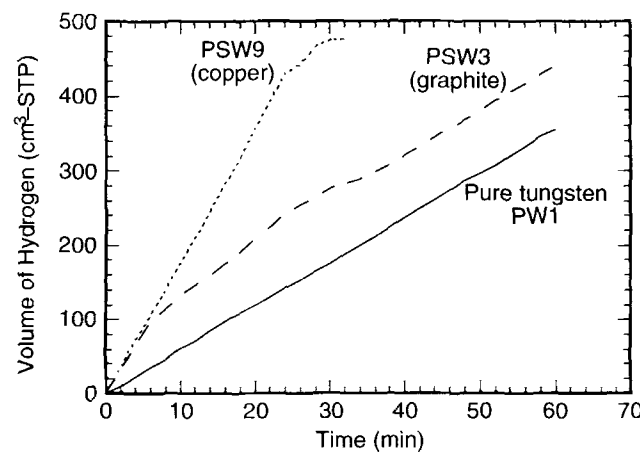


Fig. 3 Plots of hydrogen generation versus time for tungsten tested at 1100 °C.

Table 3 Experimental results from steam tests on tungsten

Sample	Temperature, °C	Total tungsten collected(a), g	Tungsten collected in filter(a), g	Flux, g/m² · s	Initial hydrogen generation rate(b), (STP)/m² · s	Latter hydrogen generation rate(c), (STP)/m² · s
PSW2	800	0.0158	0.0094	0.0036	0.097	0.047
PSW5	900	0.0760	0.0541	0.018	0.073	0.016
PSW1	1000	0.2790	0.1113	0.064	0.069	0.037
PSW3	1100	1.3263	0.3074	0.30	0.18	0.084
PSW4	1200	1.3495	0.5159	1.24	0.50	0.55
PSW8	800	0.0193	0.0096	0.0039	0.042	0.009
PSW9	1100	1.2014	0.5750	0.24	0.21	0.21
PW1	1100	0.7259	0.2529	0.38	0.19	0.18

Note: (a) Assuming tungsten product is WO_3 . (b) Rate of hydrogen generation measured for the initial 10 min of the tests. (c) Rate of hydrogen generation measured after the initial 10 min or after the downward inflection in the hydrogen production plot.

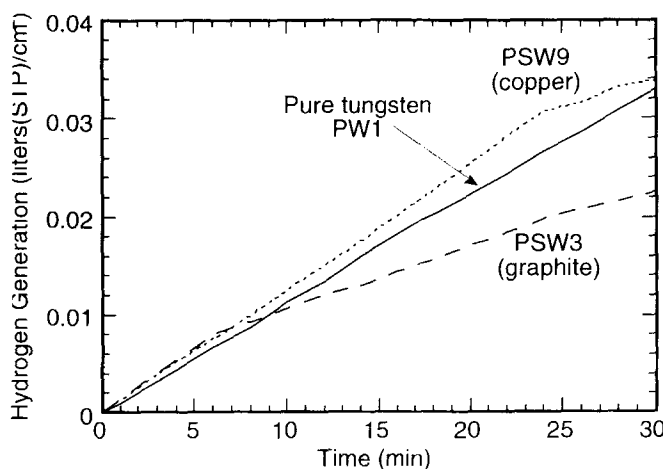


Fig. 4 Hydrogen generation per unit area for tungsten tested at 1100 °C.

measured by both methods are listed in Table 3. These results are also shown as the flux of elemental tungsten emitted from the samples in terms of $\text{g}/\text{m}^2 \cdot \text{s}$.

The amount of WO_3 deposited in the quartz wool filters appears to have influenced hydrogen measurements for some tests. The amounts of tungsten contained in the oxide collected in filters, consisting of 1 g of quartz wool packed into a 15-mm diameter tube, are included in Table 3. Larger amounts were collected in the filters during high-temperature tests. For example, 0.725 g of WO_3 (0.575 g of W) was deposited in the filter for PSW9, which was tested at 1100 °C. Complete penetration of the filters by the WO_3 was visually apparent for the tests of the plasma-sprayed samples at 1100 and 1200 °C. The WO_3 blocked some of the gas flow and probably caused some leakage and loss of hydrogen. This blockage is responsible for the departure from linear release rates of hydrogen for the plasma-sprayed samples tested at 1100 °C, as shown in Fig. 3. In fact, PSW9 was terminated after 32 min due to the sudden departure from the initial linear behavior. The sample of pure hot rolled tungsten was smaller in size; thus the amount of volatilized product was less. The filters would be less likely to become blocked and cause the system to leak. In agreement with this explanation, the plot for the pure tungsten is continuous and appears linear.

Hydrogen generation has been normalized with regard to surface area for the two forms of tungsten tested at 1100 °C. These release rates are shown in Fig. 4. The pure hot rolled and both types of plasma-sprayed tungsten exhibit similar rates during the first 10 min (Table 3). Subsequent decreases in hydrogen generation rates for the plasma-sprayed samples were probably caused by leakage, as discussed above.

Plots of hydrogen generation for deposits produced by plasma spraying onto graphite are shown in Fig. 5 for temperatures ranging from 800 to 1200 °C. For most of the plasma-sprayed samples, the slope changed after approximately 100 cm^3 of gas was collected. This initial high rate region may result from the rapid reaction of the surface layer. Initial contributions from residual argon being purged from the test system is another possibility. However, such behavior was not observed for the hot rolled tungsten.

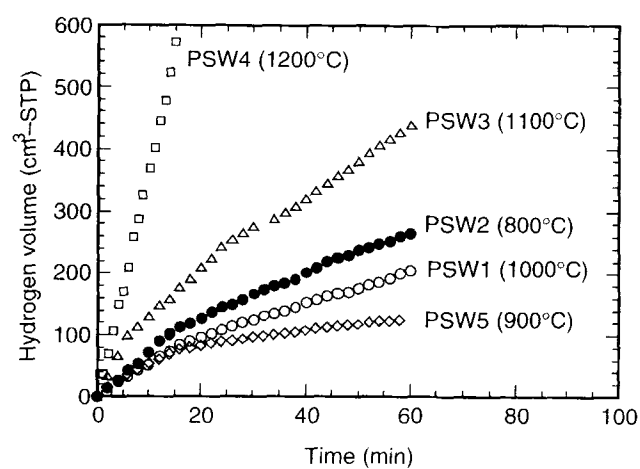


Fig. 5 Hydrogen production at various temperatures from deposits plasma sprayed onto graphite substrates.

Another observation is that the plots do not systematically increase with temperature. The plot for the 800 °C test (PSW2) lies above the plots for 900 and 1000 °C tests. This inversion may be due to different kinetics of scale development, with a more protective scale developing at 900 °C than at 800 °C. However, as temperatures increase, along with higher volatilization rates of the $\text{WO}_2(\text{OH})_2$ complex, the oxide scale becomes less protective. Such temperature trends occur in the oxidation kinetics of niobium.^[4] Similar anomalies have also been reported for the oxidation rates of tungsten in air^[5] and were believed to be caused by allotropic transformations in WO_3 . The observations reported here are based on a single set of tests and should be considered tentative. Some additional tests would be beneficial in confirming both of the trends discussed above.

3.4 Thermal Conductivity Measurements

The room-temperature thermal diffusivity of 16 free-standing tungsten disks with 12.7-mm diameters and 2.0-mm thicknesses were measured at Virginia Tech in Blacksburg, VA, using the laser flash diffusivity method. Nine of the specimens were sprayed onto stainless steel substrates (PSW-SS) and seven onto copper (PSW-Cu). One of each of these specimen types had its thermal conductivity measured from room temperature to 1500 °C (SS1500 and Cu1500).

In the flash method a pulse of thermal energy is supplied to the front surface of a thin, disk-shaped specimen by a laser or flash lamp. The pulse duration is small compared to the time required for the energy to pass through the specimen. The temperature as a function of time is recorded at the rear of the specimen, and the thermal diffusivity, D , is calculated by

$$D = 1.37 \frac{x^2}{\pi^2 t_{1/2}} \quad [1]$$

where x is the specimen thickness, and $t_{1/2}$ is the time required for the back face to reach half its maximum temperature. The accuracy was 3 to 4% at room temperature and 5% at elevated temperatures.

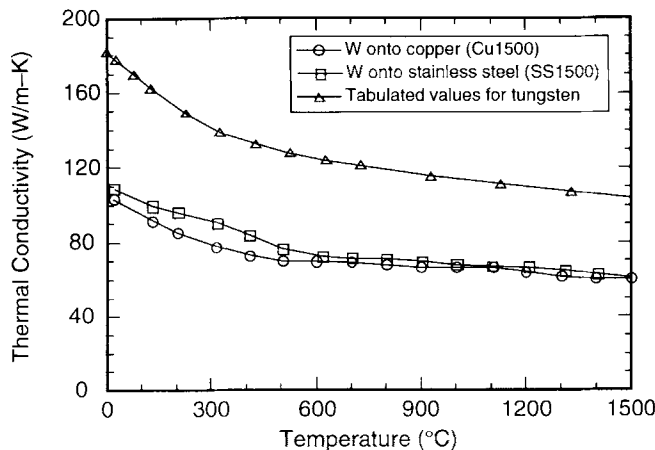


Fig. 6 Thermal conductivity as a function of temperature for plasma-sprayed tungsten. Tabulated values for high-purity, well annealed tungsten are also shown.

To calculate thermal conductivities, the sample density and heat capacity are required, as shown in the expression:

$$\kappa = \rho C_p D \quad [2]$$

where κ is the thermal conductivity; ρ is the density; and C_p is the heat capacity. The average density of both the PSW-Cu and PSW-SS samples was 17.5 g/cm³. The specific heat of tungsten as a function of temperature was taken from Ref 6.

The thermal conductivities at room temperature were all very similar. The mean value for PSW-SS was 107.0 W/m · K with a standard deviation of 2.3. The PSW-Cu specimens had a mean of 106.3 W/m · K and a standard deviation of 9.2. The cause of the larger scatter in the thermal conductivity values for the deposits sprayed onto copper is not known.

At the time of publication, the authors became aware of recent work by Moreau et al. that reports the thermal diffusivity of tungsten plasma sprayed at atmospheric pressure.^[7] They obtained the highest thermal diffusivity when the spraying was performed in an inert atmosphere. However, the maximum value they measured, 0.13 cm²/s, is considerably smaller than those reported here for vacuum plasma-sprayed coatings (typically 0.45 cm²/s). The reason for the difference is uncertain, but the much higher substrate temperatures during vacuum plasma spraying may play a role.

The thermal conductivity of the plasma-sprayed tungsten at elevated temperatures is shown in Fig. 6. Except for a slightly higher conductivity in SS-1500 from 100 to 400 °C, the two plasma-sprayed coatings were essentially the same. The temperature dependence of the plasma-sprayed tungsten is very similar to tabulated values for high-purity, well annealed tungsten.^[8] A ratio of the thermal conductivities of the plasma-sprayed and well annealed, high-purity tungsten was taken. Over the temperature range 25 to 1500 °C, the thermal conductivity of low-pressure plasma-sprayed tungsten is approximately 60% of the value measured for high-purity tungsten.

After the two sprayed specimens had been heated to 1500 °C, their room-temperature thermal conductivities were remeasured. For Cu-1500, κ rose from 103.3 W/m · K before the test to 145.7 W/m · K after. However, SS-1500 dropped from 108.7 to 86.9 W/m · K. It was noted that SS-1500 had become slightly



Table 4 Elastic constants of plasma-sprayed tungsten

	W on Cu	W on stainless	Isotropic W
E_{11} , GPa	304.8	298.2	408.6
E_{33} , GPa	283.3	280.0	...
G_{13} , GPa	113.4	111.2	160.2
G_{12} , GPa	117.0	116.2	...
v_{12}	0.30	0.28	0.28
v_{13}	0.22	0.22	...
v_{31}	0.21	0.21	...

dome shaped during the test. Bulk density measurements were made on the two heated specimens both before and after the test. No change in density was observed.

3.5 Ultrasonic Examination

The elastic constants were determined ultrasonically for one of the PSW-Cu specimens and for one of the PSW-SS specimens. Table 4 lists the measured values. The 1 and 2 directions are in the plane of the deposit, whereas direction 3 is perpendicular to the surface of the deposit (parallel to the spray axis). The table also shows the isotropic tungsten values for Young's modulus, the shear modulus, and Poisson's ratio. The specimens were assumed to be isotropic in the plane of the specimen, i.e., in the 1-2 plane.

The elastic properties of the two plasma-sprayed specimens are very similar. Both exhibit anisotropy and are about 7% stiffer in the plane of the deposit than perpendicular to it. The shear moduli and Poisson's ratio are also anisotropic. As compared to the isotropic values reported for tungsten, the moduli of the sprayed tungsten were approximately 30% lower.

The anisotropy is a consequence of the microstructure of a plasma-sprayed deposit. A plasma-sprayed material should not be as stiff in the direction perpendicular to the substrate as it is in the direction parallel to the substrate because of the poor contact between the flattened droplets. That the anisotropy is not greater is possibly because of the large quantity of unmelted material observed in Fig. 1, which makes the microstructure more isotropic.

The longitudinal velocity of sound was measured in four specimens along the 3-axis, perpendicular to the specimen surface. One each of PSW-Cu and PSW-SS were tested along with Cu-1500 and SS-1500. The two specimens that had been heated (Cu-1500 and SS-1500) had higher velocities than the two as-sprayed specimens (PSW-Cu and PSW-SS). This increase indicates that some sintering occurred during heating, resulting in improved bonding between splats. SS-1500 had a velocity of 4.91 mm/μs and the velocity of Cu-1500 was 4.65 mm/μs. The as-sprayed specimens had longitudinal velocities of 4.32 for PSW-SS and 4.20 mm/μs for PSW-Cu.

4. Discussion

4.1 Steam Tests

Volatilization rates in steam did not exhibit a dependence on the product form, i.e., no difference between hot rolled and plasma-sprayed tungsten. According to Hastie, volatilization occurs by the $\text{WO}_2(\text{OH})_2$ complex.^[9] This species is unstable

and decomposes to WO_3 . Chemical analysis of the product that was deposited on a downstream component yielded 79.3 wt% tungsten and confirmed that it was WO_3 . Fluxes for the two types of plasma-sprayed deposits and hot rolled tungsten at 1100 °C (shown in Table 3) all range from 0.24 to 0.38 $\text{g/m}^2 \cdot \text{s}$. Volatilization rates in Table 3 also agree with rates previously reported for an experimental tungsten alloy.^[10] This alloy, containing small additions of nickel, rhenium, iron and cobalt, was formed by liquid-phase sintering. The rates at 800, 1000, 1100, and 1200 °C were 0.0033, 0.044, 0.22, and 0.82 $\text{g/m}^2 \cdot \text{s}$, respectively. These rates generally agree within 50% to the tests in the current investigation. The volatilization process is apparently controlled by the reaction that forms the hydroxide complex. There are sufficient supplies of tungsten oxide to establish this complex irrespective of the product form.

A comparison of the reaction rates of the hot rolled and plasma-sprayed tungsten, as indicated by hydrogen generation, is shown in Fig. 4. Within the initial 10 min, during which there was no evidence of hydrogen leakage, the observed rates for the two types of plasma-sprayed deposits and the hot rolled tungsten were essentially equivalent. The effective surface areas of the plasma-sprayed deposits were not significantly increased by any surface porosity or smaller microporosity within the deposits. Steam apparently does not significantly penetrate into the deposits. In conclusion, steam reacts with plasma-sprayed tungsten at rates comparable to those of pure, fully dense tungsten.

4.2 Thermal Conductivity Measurements

The conduction of heat through a metallic body is strongly affected by the presence of internal surfaces and voids. Looking at the microstructure in Fig. 1, it is not surprising that the conductivity of the sprayed deposits is lower than the tabulated values for high-purity well-annealed tungsten.

Exposing the tungsten to 1500 °C should allow for some diffusion because this is about one half of its melting point. During the short time required to make the thermal diffusivity measurement, it seems that it was possible for enough diffusion to take place to significantly close any of the large pores visible in Fig. 1, because the density of the two heated specimens (SS-1500 and Cu-1500) remained unchanged by the exposure. However, the higher velocities of sound in the two heated specimens and the higher κ value at room temperature for Cu-1500 indicate that some improvement in splat bonding did take place. These data could be explained by diffusion across splat boundaries. The diffusion distances are short, and improved bonding should raise both κ and the velocity of sound without affecting the bulk density.

The drop in the room-temperature conductivity observed in SS-1500 could not be explained. Warpage observed in the specimen may have created some internal flaws in the brittle tungsten. These would reduce the thermal conductivity at room temperature. Because both SS-1500 and Cu-1500 show the same behavior up to 1500 °C in Fig. 6, it seems reasonable to conclude that whatever caused the loss of thermal conductivity in SS-1500 happened during cooling. An ultrasonic examination of the specimen revealed an internal flaw, but it did not seem to be big enough to cause the large drop in κ . However, a tightly closed crack may escape ultrasonic detection, but still significantly reduce thermal conductivity. The residual internal

stresses developed in the deposit during spraying, coupled with the thermal stresses caused by heating the specimen to 1500 °C, may have caused the warpage of SS-1500. Plasma-facing components inside fusion reactors like ITER will be exposed to high temperature gradients and cyclical heat loads. The results of these tests indicate that such conditions could potentially cause cracking and/or delamination in deposits or coatings. Further work should therefore be performed to examine the properties of plasma-sprayed tungsten under conditions of cyclic thermal stresses.

5. Conclusions

There are no significant differences between hydrogen generation rates, in terms of liters per square meter per second, resulting from steam reactions with plasma-sprayed tungsten deposits having densities 90% of theoretical and fully dense, pure, hot rolled tungsten. Volatility of tungsten by means of the oxidation product $\text{WO}_2(\text{OH})_2$ was not dependent on the form of tungsten tested in this investigation. The plasma-sprayed deposits prepared on graphite and copper, hot rolled tungsten, and a tungsten alloy^[9] all exhibited similar volatility in terms of grams, $\text{W/m}^2 \cdot \text{s}$. The thermal conductivity of the plasma-sprayed tungsten was approximately 60% of the tabulated value for high-purity, well annealed tungsten room temperature to 1500 °C. The low value is due to the lower density (90% of the theoretical) and splat microstructure of the sprayed material.

An increase in the room-temperature thermal conductivity in Cu-1500 after exposure to 1500 °C and an increase in the velocity of sound in both Cu-1500 and SS-1500 indicate that some inter-splat diffusion occurred during the heating cycle. The decrease in room-temperature thermal conductivity and the warpage that was observed in SS-1500 after heating to 1500 °C indicate the need for further testing of plasma-sprayed tungsten under conditions of cyclic temperature loading. The elastic moduli of the plasma-sprayed deposits were approximately 30% lower than the tabulated values for isotropic tungsten. There was a noticeable anisotropy in the elastic properties of the sprayed tungsten in the directions parallel and perpendicular to the specimen surface.

Acknowledgments

The authors would like to thank R. Cote for his assistance in plasma spraying the specimens examined in this study and J. Gieseke for measuring their elastic properties. One of the authors (KH) would like to recognize support from the Magnetic Fusion Energy Technology Fellowship Program administered by Oak Ridge Associated Universities for the US Department of Energy. The work performed at Sandia National Laboratories and at Idaho National Engineering Laboratory was supported by the Department of Energy under contract numbers DE-AC04-76DP00789 and DE-AC07-76ID01570, respectively.

References

1. C. Moreau, P. Cielo, and M. Lamontagne, Flattening and Solidification of Thermal Sprayed Particles, *J. Thermal Spray Technol.*, Vol 1 (No. 4), 1992, p 317-324



2. S. Sampath, "Rapid Solidification During Plasma Spraying," Ph.D. thesis, State University of New York at Stony Brook, 1989
3. G.R. Smolik and K.A. McCarthy, "Oxidation and Volatilization of a Niobium Alloy," EGG-FSP-10341, July 1992
4. J.N. Ong, Jr. and W.M. Fassell, Jr., Kinetics of Oxidation of Columbium and Other Refractory Metals, *Corrosion*, Vol 18, 1962, p 382-389
5. V.D. Barth and G.W.P. Rengstorff, "Oxidation of Tungsten," DMIC Report 155, June 1961
6. Specific Heat, in *Metallic Elements and Alloys*, Vol 4, TRPC Data Series, Plenum, 1973, p 263-267
7. C. Moreau, P. Fargier-Richard, R.G. Saint-Jacques, and P. Cielo, Thermal Diffusivity of Plasma-Sprayed Tungsten, *Surf. Coat. Technol.*, to be published
8. Thermal Conductivity, in *Metallic Elements and Alloys*, Vol 1, TPRC Data Series, Plenum, 1970, p 415
9. J.W. Hastie, *High Temperature Vapors*, Academic Press, 1975, p 62-68
10. G.R. Smolik, S.J. Piet, and R.M. Neilson, Jr., Predictions of Radioactive Tungsten Release for Hypothetical ITER Accidents, *Fusion Technol.*, Vol 19, 1991, p 1398-1402